Proceedings of the International Symposium on Physics of Materials (ISPMA13)

Interrelation of Microstructure and Corrosion Resistance in Biodegradable Magnesium Alloys with Aluminum, Lithium and Rare Earth Additions

P. Minárik[a], M. Landa[b], I.K. Lesná[c], M. Zemková[a], E. Jablonská[d], B. Hadzima[e], M. Janeček[a] and R. Král[a,*]

[a]Charles University in Prague, Department of Physics of Materials, Ke Karlovu 5, Prague 2, CZ-12116, Czech Republic

[b]Academy of Sciences of the Czech Republic, Institute of Thermomechanics, Prague, Czech Republic

[c]Institute of Clinical and Experimental Medicine, Prague, Czech Republic

[d]University of Chemistry and Technology, Department of Biochemistry and Microbiology, Prague, Czech Republic

[e]Research Center of the University of Žilina, Žilina, Slovak Republic and Faculty of Mechanical Engineering, University of Žilina, Žilina, Slovak Republic

The influence of equal channel angular pressing and rotary swaging on the microstructure and corrosion resistance was investigated in three magnesium alloys with the addition of aluminum, lithium and rare earth elements — AE21, AE42 and LAE442. The processing resulted in grain refinement in all cases; nevertheless, the effect on the corrosion resistance was ambiguous. A continuous increase of the polarization resistance during the gradual equal channel angular pressing was observed in the AE42 and LAE442 alloys, whereas there was almost no effect in the AE21 alloy. The rotary swaging of AE42 resulted in a decrease of polarization resistance. The increase of polarization resistance in the alloys with the higher concentration of alloying elements was caused by the combined effect of grain refinement and better dispersion of particles in the matrix thanks to shear deformation during equal channel angular pressing. In the AE42 alloy, the increase of the corrosion resistance after equal channel angular pressing was also proven by chemical analysis of the solution and acoustic emission detection. This beneficial effect was not observed when the concentration of alloying elements was lower or when the deformation mode was different from shearing.

DOI: 10.12693/APhysPolA.128.491

PACS: 81.05.–t, 82.45.Bb, 87.85.J–, 43.40.Le

1. Introduction

Magnesium alloys are a very attractive material for structural components due to their excellent strength to weight ratio. At present time, magnesium alloys are commonly used in the automotive industry, but their biocompatibility and biodegrability also provide possibilities for biomedical applications, such as e.g. degradable stents or bone fracture fixation pins [1–5]. For a successful application of magnesium as a biodegradable material, the following issues are critical:

- The lifetime of the implant;
- The strength during the degradation period;
- The corrosion resistance;
- The non-toxicity as a prerequisite for biocompatibility and biodegradability;
- The osteoconductivity.

*corresponding author; e-mail: robert.kral@mff.cuni.cz

Concerning the first three issues, the possible ways to achieve favorable properties are similar and related to the manipulation of the (i) composition of the alloys and (ii) the microstructure of the material. The surface treatment is not suitable for the control of the corrosion rate in this case, as a constant rate has to be maintained in the whole implant during the degradation period. The last two issues are strongly connected to the composition of the alloy and therefore the investigated alloys should be selected very carefully.

After Heublein successfully tested an AE21 coronary stent in domestic pigs in 2003 [1], the research in the field of bio-implants began to develop significantly and new types of the alloys were needed. In this field of application, superior properties were found in the magnesium alloys containing rare earths (E). Today's alloys with the top properties from the *in vivo* tests are WE43 and LAE442, containing yttrium (W) and lithium (L) [2–4, 6]. The AE42 alloy is a commercially successful high temperature creep resistant alloy [7] and is considered for studying because it is an interstage between the LAE442 and AE21 alloys.

AE type alloys (AE21, AE42) are well-known alloys with a documented microstructure. Both aluminum and rare earth additions improve the mechanical properties

and support grain refinement [8]. Furthermore, the rare earth component improves the creep resistance. The presence of aluminum and rare earth elements provides dispersoids of $Al_{11}RE_3$ that reduce the mobility of grain boundaries and stabilize the fine-grain structure [9]. These alloys were also reported as being suitably deformable and corrosion resistant [10]. An even better corrosion resistance has been reported for LAE alloys with the addition of lithium [11], but the microstructure and mechanical properties have not been investigated yet.

The discussion about aluminum as a suitable alloying element for the magnesium-based biodegradable implants is still vital. There is a connection between aluminum and Alzheimer's disease, but the degradation rate of the implant is necessarily very low, and therefore the doses of aluminum should also be negligible. There are papers showing no negative effect of magnesium-based implants with an aluminum addition. Moreover, enhanced osteoblastic activity was reported when the weight percentage of the aluminum in the magnesium alloy was not exceeding 9% [11, 12].

The corrosion layer that develops on the surface of the material is crucial for its corrosion properties. In the case of larger degradable implants, it is not possible to increase the corrosion resistance by a deposition of a protective layer since such a layer would either stop the degradation completely or, in case of its eventual failure, the degradation rate would be uncontrolled. The latest research showed another way to enhance the corrosion resistance in magnesium based alloys — to achieve an ultrafine-grained (UFG) microstructure. The strength of UFG materials can be 2–3 higher than that of materials with large ($d > 50$ μm) grains and simultaneously, their good workability remains unchanged or is even improved after the grain refinement. In some cases, the grain refinement was also reported to improve the corrosion resistance. There are, in principle, two ways to produce a material with UFG structure: (i) from an atomized material or (ii) by thermomechanical processing. In the second case, the methods of severe plastic deformation (SPD) are very effective.

Many SPD techniques have been developed. The equal channel angular pressing (ECAP), first reported by Segal [13], is one of the most extensively used SPD techniques. The sample, in the form of a rod or bar, is machined to fit within the channel and the die is placed in some form of press so that the sample can be pressed through the die using a plunger. Shear deformation is introduced into the sample since the channel is bent inside the die. Rotary swaging (abbreviated as RS) is another forming process originally designed for reducing cross-sections of rod and tube materials in many industrial applications [14]. Recently, it attracted the interest of researchers as it allows processing rods of pure magnesium and magnesium alloys more efficiently than the classical die-casting and extrusion. The main reason is the lower temperature and higher velocity of processing as compared to the extrusion [15, 16]. By optimizing the processing conditions of RS (temperature, feeding velocity) one may attain even finer-grained microstructure than by direct or indirect extrusion [17]. Our earlier study indicated enhanced strength without substantial deterioration of ductility and enhanced fatigue properties in RS ZK60 alloy as compared to ECAP processed material [18].

The ECAP processing was found to increase the corrosion resistance in AZ31 and ZE41A magnesium alloys [19, 20] and AE42 alloy [21, 22]. In contradiction to these results are papers reporting that ECAP processing weaken the corrosion resistance with increasing number of routes, e.g. [23]. The ideal example of such a controversy are two papers, both reporting evolution of the corrosion resistance of pure magnesium in NaCl aqueous solution, where the first reported an increase of corrosion resistance and the second one a diminishing corrosion resistance with the increasing number of ECAP passes [24, 25]. The relation of microstructure to the corrosion properties is a complicated problem which still has to be solved. The aim of this paper is to contribute to the understanding of these phenomena.

2. Experimental methods

Three magnesium alloys with a potential for biomedical applications were investigated in this study: AE21, AE42 and LAE442. The alloys were extruded at the temperature of $T = 350\,^{\circ}\mathrm{C}$ and the extrusion ratio of $ER = 22$. The billets for ECAP, with the initial dimensions of 10 mm $\times$ 10 mm $\times$ 100 mm, were machined from the extruded bar. ECAP processing was carried out up to twelve passes (12P) following route B_c. The angle between two intersecting channels was 90°. The processing was performed between 185–230 °C at the rate of 5–10 mm/min. In the case of the AE42 alloy, the second part of the extruded rods was swaged at an initial temperature of 250 °C. A 4-hammer rotary swaging system was used. Swaging was performed in 5 steps with an intermediate 5 min reheating. During swaging, the as-extruded diameter was reduced from 16 to 7.5 mm.

The microstructure after ECAP processing was studied with the scanning electron microscope (SEM) FEI Quanta equipped with the EDAX EBSD camera. The specimens were cut from the billet with the investigated surface perpendicular to the processing direction. The samples were mechanically polished with a grain size decreasing down to 0.25 μm and afterwards ion polished using the Gatan PIPS™ ion mill.

The effect of ECAP processing on the corrosion resistance was investigated by the linear polarization method. The measurements were performed using a three-electrode setup and controlled by the potentiostat AUTOLAB128N. The samples were cut perpendicular to the processing direction and the exposed surface was ground with 1200 grit emery paper before each measurement. The measurements were performed in the 0.1 M NaCl solution with an initial pH of 7 after five minutes of stabilization. The characteristics were measured

in the potential range from −150 mV to 200 mV with respect to open circuit potential (OCP) with a constant scan rate of 1 mV s^{-1}. Additional rotation of 300 rpm was introduced to the sample to provide better homogeneity of the measurement. At least three measurements were performed for each sample/condition.

Corrosion resistance was also investigated using immersion tests. Samples of AE42 with and without ECAP treatment were immersed into simulated body fluid (SBF), pH 7.4 prepared according to Kokubo and Takadama [26] and agitated at 37 °C and 125 rpm for one week in closed vessels. Surface to volume ratio was 2 mm^2 per 1 ml. Triplicates were used for all types of samples. Thereafter, concentration of magnesium in the extracts was measured using atomic absorption spectrometry.

The corrosion processes during the layer formation in the same solution were further investigated by acoustic emission (AE) method. The AE response was monitored using a computer controlled DAKEL-CONTI-4 system on the basis of four channel acquisition (with different amplification) which allows continuous sampling (with the frequency of 2 MHz) of the AE signal registered by a 6 mm piezoelectric transducer MIDI-410-02 with a frequency band 100–600 kHz. This makes possible a comprehensive post-processing of the complete stored signal based on a standard two-threshold level detection (recommended by ASTM standard E1067-85) using various parameters of individualization of the AE events [27]. Further information on the analysis of signal and AE parameters can be found in [28, 29].

Cytotoxicity measurement provided the information how much the studied specimens are toxic to human body. Cytotoxicity was studied *in vitro* on the cell lines. There were used THP-1 human monocytes (human monocytic leukemia cells, ECACC 88087201), which were maintained in RPMI 1640 medium containing 10% fetal bovine serum, 2 mM glutamine and 1% penicillin/streptomycin (PAA Laboratories) at 37 °C, 5% CO_2. Before experiments THP-1 monocytes were seeded into 12-well plates at a density approximately 5×10^5/ml. Measurement was performed by determination of the cell viability using the trypan blue dye exclusion method (Vi-CELL, Cell Viability Analyzer, Beckham Coulter). The cell culture model does not completely reflect the situation *in vivo* where numerous physiological mechanisms are involved, but the cell model used has been repeatedly proven to be a good approximation of the situation in the tissues [30].

3. Results and discussion

The microstructure after extrusion in all three investigated alloys was documented by EBSD and the results are presented in Fig. 1. The extrusion conditions were the same for all three alloys; however, a difference was observed between the AE-group and the LAE442 alloy. Grain size distribution in the AE21 and the AE42 alloy exhibited a bimodal character with a high area fraction of small grains of ≈ 3−6 μm in diameter, see Fig. 1a and b. This indicates that in these alloys, the microstructure resulted from partial dynamic recrystallization [31]. On the other hand, the LAE442 alloy was formed by recrystallized equiaxed grains of an average size of 20−40 μm, see Fig. 1c.

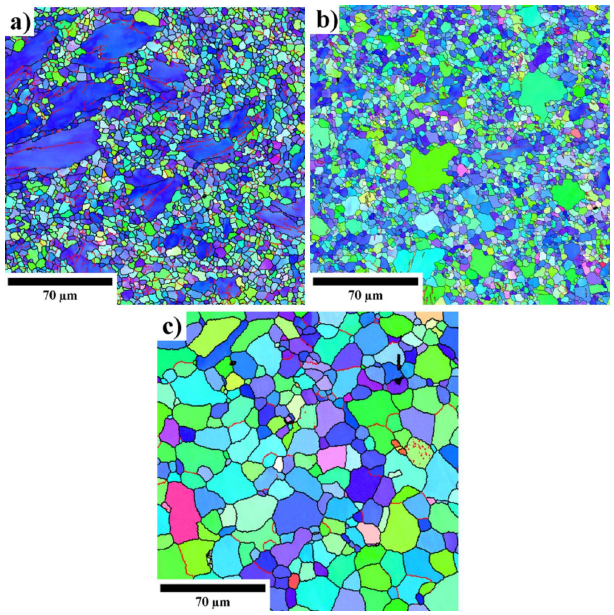

Fig. 1. EBSD micrographs of the extruded samples (a) AE21, (b) AE42, (c) LAE442.

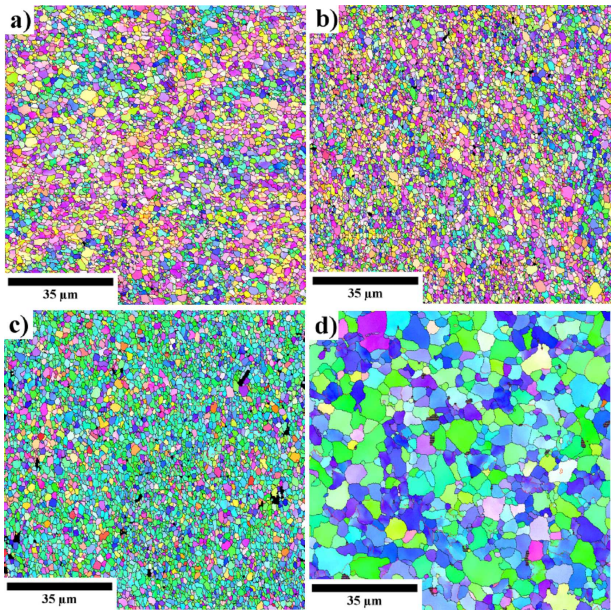

Fig. 2. EBSD micrographs after ECAP processing (a) AE21, (b) AE42, (c) LAE442 and after RS (d) AE42.

The processing by ECAP led to a significant grain refinement with the resulting average grain size of ≈1.5 μm in all three investigated alloys, as depicted in Fig. 2. The average grain size in the refined condition is com-

parable to other magnesium alloys processed in the same way, see e.g. [32]. In case of AE42 alloy, the processing by RS did not result in such a grain refinement as observed after ECAP. Moreover, the microstructure was not homogeneous through the cross-section of the rods. The processing resulted in grain size homogenization in the central area with the average grain size of ≈5 μm (Fig. 2d), whereas the average grain size in the peripheral area was ≈2 μm [33]. The rotary swaging of the LAE442 alloy resulted in substantial segmentation of the material, and therefore it is not part of this study.

The average grain size and fraction of high angle boundaries were calculated from the EBSD data. It should be noted in Fig. 3a that major grain refinement was observed after the first pass through ECAP in both AE-type alloys, but in the LAE442 alloy, the grain refinement occurred gradually within the first four passes. This difference resulted from the initial microstructure (as-extruded), where a substantially higher grain size was observed in the LAE442 alloy [34]. The evolution of high angle grain boundaries (HAGB) is shown in Fig. 3b. The HAGB were considered as boundaries with a misorientation angle higher than 15° [35]. In all studied conditions (ECAP, RS), the length fraction of HAGB was very high, which indicates a high degree of recrystallization. In AE42 and LAE442, a typical decrease of the HAGB fraction was observed after the first ECAP pass, which is associated with grain fragmentation [32]. In the AE21 alloy, such decrease was not observed as a result of a lower fraction of HAGB in the as-extruded condition, which is a consequence of the fact that only partial dynamic recrystallization took place during the processing.

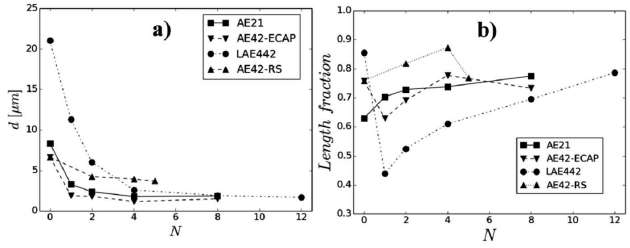

Fig. 3. Evolution of (a) average grain size and (b) length fraction of HAGB on the increasing stage of processing.

The corrosion resistance of the investigated alloys was studied by linear polarization measurement. This method was used to estimate the initial corrosion attack immediately after immersion into a 0.1 M NaCl solution. The resulting polarization resistance R_P was calculated according to the Stern–Geary method. The linear fit near the corrosion potential (E_0) of all investigated conditions is shown in Fig. 4.

The evolution of the calculated polarization resistance is presented in Fig. 5. In case of the AE21 alloy, the tests showed almost no difference between the extruded samples and the samples after ECAP processing. On the

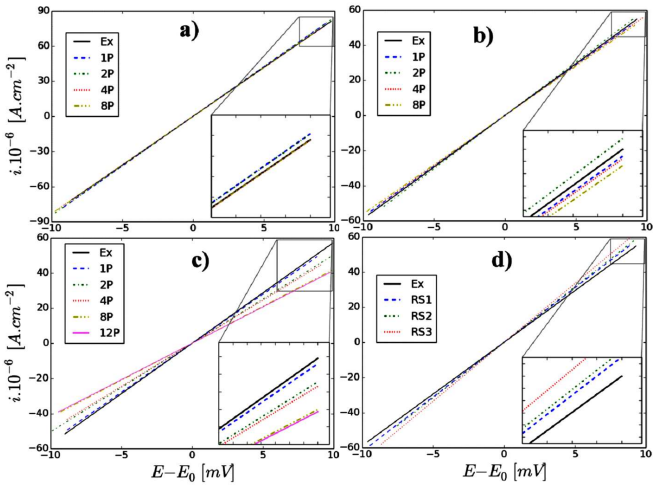

Fig. 4. Linear fit near E_0 ($i = 0$ Acm^{-2}) of the linear polarization data: (a) AE21, (b) AE42-ECAP, (c) LAE442, and (d) AE42-RS.

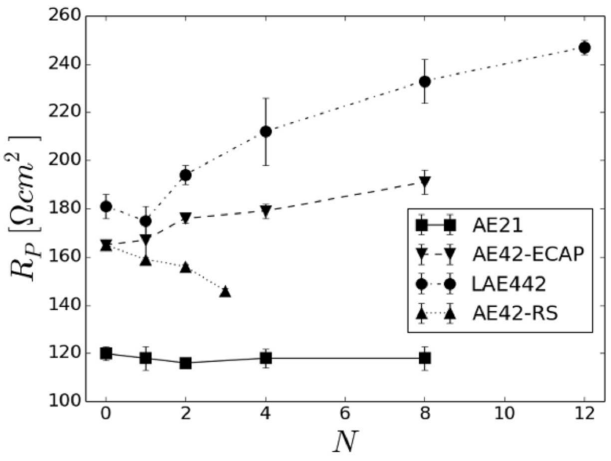

Fig. 5. Evolution of the polarization resistance R_P calculated from Fig. 4. ($R_P = 1/\text{slope}$).

other hand, an evolution of the polarization resistance was observed in the AE42 and LAE442 alloys, where a continuous increase was found with the gradual ECAP processing. Finally, the RS processing of AE42 resulted in a decrease of polarization resistance from 165 to 146 Ω cm^2.

The increase of polarization resistance in the alloys with higher concentration of alloying elements is caused by better dispersion of alloying elements in the matrix [22]. In these alloys, there is present an aluminum rich phase ($Al_{11}RE_3$) in the form of secondary phase particles, which are fragmented and dispersed in the matrix by the shear deformation during ECAP [13, 22]. Better distribution of alloying elements together with smaller grain size resulted in faster formation of a more stable corrosion layer that suppressed further corrosion. Better distribution of secondary phase particles is depicted in Fig. 6, where a comparison of AE42-Ex and AE42-8P samples surface after 15 days of immersion is shown.

After the extrusion, the secondary particles are aligned in stripes parallel to the processing direction (red ellipse marks), which are not observed after ECAP. Moreover, the corrosion layer after ECAP is stiffer and composed of smaller segments.

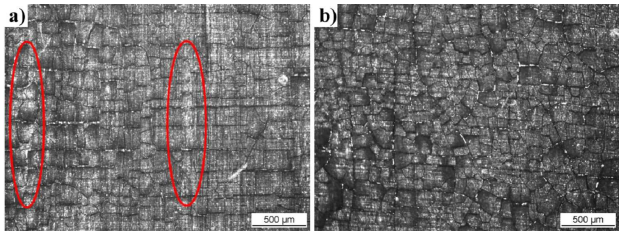

Fig. 6. Comparison of the corrosion layer formed on the (a) AE42-Ex and (b) AE42-8P after 15 days immersion. The red ellipses mark the region rich on $Al_{11}RE_3$ particles.

In the case of RS, the deformation mode is different from shearing and the dispersion of particles was not substantially affected. The lower polarization resistance observed in AE42 after RS supports the conclusion that the distribution of alloying elements considerably affects the resulting corrosion resistance.

Higher corrosion resistance of the AE42 alloy processed by ECAP is also supported by results acquired after a long time immersion in SBF. The corrosion rate after 7 days of immersion was estimated according to the concentration of magnesium ions in the solution. The results showed that the corrosion rates of the AE42 alloy in the as-extruded condition and after the final stage of ECAP were (1.21 ± 0.07) mg/cm^2/day and (1.09 ± 0.03) mg/cm^2/day, respectively. Higher corrosion resistance of the alloy in the condition after ECAP in the NaCl and SBF solutions points to a general increase of the corrosion resistance. Therefore, it is likely that a similar increase could also be expected in the *in vivo* case.

A similar positive effect of ECAP was recently also found in other types of materials, e.g. aluminum alloys [36]. In coarse-grained AA6061 aluminum alloy, selective corrosion of the individual grains was observed, leading to the formation of deep and large pits on the sample surface. The ECAP processing led to the formation of a shallow and uniformly corroded surface [36]. On the other hand, the lower polarization resistance observed in AE42 after RS seems to be in contradiction with the results for aluminum [37] where an improved corrosion resistance was observed after swaging. Nevertheless, this difference can be explained by fast passivation of the surface in the case of aluminum, contrary to magnesium, where the layer needs to be stabilized by alloying elements.

Comparing the viability of THP-1 human monocytes in the initial condition (95.4%) and the condition after 24 h of exposure to AE42 samples (89.1% and 92.2% viability for the as-extruded and ECAP states, respectively), it can be concluded that the ECAP processing of the AE42 alloy resulted in substantially lower toxicity for the cells, compared to the as-extruded samples. Since the composition was the same, the difference in toxicity can be attributed to the lower corrosion rate of the AE42 alloy processed by ECAP.

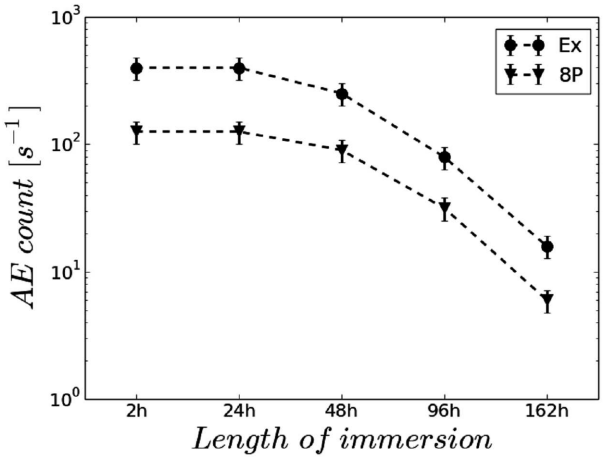

Fig. 7. Comparison of the AE count rate for the AE42 after extrusion and eight passes through ECAP during long term immersion.

Acoustic emission related to the progress of corrosion [38] was detected during a long term immersion of AE42 after extrusion and ECAP in a 0.1 M NaCl solution with a pH of 7. The time dependence of acoustic activity of both samples is shown in Fig. 7. For all immersion lengths, the AE activity was lower by a factor of $\approx$2.5 for the ECAP state compared to the extruded state, which confirms a better corrosion resistance in AE42 after ECAP. The decrease of AE activity in time for both the as-extruded and the ECAP states is due to the gradual formation of a protective surface layer [19, 22]. The AE measurements thus fully testify the results of both the linear polarization and cell viability tests.

4. Conclusions

1. In all three alloys, fine-grained microstructure was achieved after SPD. The ECAP processing had almost no effect on the corrosion resistance of the AE21 alloy. On the other hand, in the AE42 and LAE442 alloys, an increase of corrosion resistance with the increasing number of ECAP passes was observed. The RS processing of AE42 resulted in a decrease of corrosion resistance. The concentration of Mg ions in the solution, the AE count rate and the toxicity for THP-1 human monocytes decreased in AE42 after ECAP.

2. In the AE42 and LAE442 alloys, better distribution of Al containing dispersed particles resulted in a better corrosion resistance of the fine-grained microstructure when compared to the extruded material. This beneficial effect was not observed in the

case of the AE21 alloy with a lower concentration of alloying elements and in the case of RS processing where the dispersion of particles was not substantially affected due to the fact that the deformation mode was different from shearing.

Acknowledgments

The present work is a part of the Czech Grant Agency project no. 14-36566G. B.H. acknowledges the financial support from the European Regional Development Fund and the Slovak state budget under the project with the ITMS code 26220220183.

References

[1] B. Heublein, R. Rohde, V. Kaese, M. Niemeyer, W. Hartung, A. Haverich, *Heart* **89**, 651 (2003).

[2] A. Krause, N. von der Höh, D. Bormann, C. Krause, F.-W. Bach, H. Windhagen, A. Meyer-Lindenberg, *J. Mater. Sci.* **45**, 624 (2010).

[3] F. Witte, J. Fischer, J. Nellesen, C. Vogt, J. Vogt, T. Donath, F. Beckmann, *Acta Biomater.* **6**, 1792 (2010).

[4] M. Thomann, C. Krause, D. Bormann, N. von der Höh, H. Windhagen, A. Meyer-Lindenberg, *Mater. Werkst.* **40**, 82 (2009).

[5] S. Virtanen, *Mater. Sci. Eng. B* **176**, 1600 (2011).

[6] C. Di Mario, H. Griffiths, O. Goktekin, N. Peeters, J. Verbist, M. Bosiers, K. Deloose, B. Heublein, R. Rohde, V. Kaese, C. Ilsley, R. Erbel, *J. Intervent. Cardiol.* **17**, 391 (2004).

[7] T. Rzychoñ, A. Kielbus, *Arch. Mater. Sci. Eng.* **28**, 601 (2007).

[8] X. Tian, L.M. Wang, J.L. Wang, Y.B. Liu, J. An, Z.Y. Cao, *J. Alloys Comp.* **465**, 412 (2008).

[9] I.P. Moreno, T.K. Nandy, J.W. Jones, J.E. Allison, T.M. Pollock, *Scr. Mater.* **48**, 1029 (2003).

[10] F. Rosalbino, E. Angelini, S. De Negri, A. Saccone, S. Delfino, *Intermetallics* **14**, 1487 (2006).

[11] F. Witte, V. Kaese, H. Haferkamp, E. Switzer, A. Meyer-Lindenberg, C.J. Wirth, H. Windhagen, *Biomaterials* **26**, 3557 (2005).

[12] F. Witte, I. Abeln, E. Switzer, V. Kaese, A. Meyer-Lindenberg, H. Windhagen, *J. Biomed. Mater. Res. A* **86**, 1041 (2008).

[13] V.M. Segal, *Mater. Sci. Eng. A* **197**, 157 (1995).

[14] E. Rauschnabel, V. Schmidt, *J. Mater. Process. Technol.* **35**, 371 (1992).

[15] M.R. Barnett, Z. Keshavarz, A.G. Beer, D. Atwell, *Acta Mater.* **52**, 5093 (2004).

[16] T. Murai, S. Matsuoka, S. Miyamoto, Y. Oki, *J. Mater. Process. Technol.* **141**, 207 (2003).

[17] J. Bohlen, S.B. Yi, J. Swiostek, D. Letzig, H.G. Brokmeier, K.U. Kainer, *Scr. Mater.* **53**, 259 (2005).

[18] M.Z. Oo, M. Janeček, R. Kral, L. Wagner, *Acta Phys. Pol. A* **122**, 606 (2012).

[19] B. Hadzima, M. Janecek, M. Bukovina, R. Kral, *Int. J. Mater. Res.* **100**, 1213 (2009).

[20] J. Jiang, A. Ma, N. Saito, Z. Shen, D. Song, F. Lu, Y. Nishida, D. Yang, P. Lin, *J. Rare Earths* **27**, 848 (2009).

[21] P. Minárik, R. Král, B. Hadzima, *Acta Phys. Pol. A* **122**, 614 (2012).

[22] P. Minárik, R. Král, M. Janeček, *Appl. Surf. Sci.* **281**, 44 (2013).

[23] D. Song, A.B. Ma, J.H. Jiang, P.H. Lin, D.H. Yang, J.F. Fan, *Corros. Sci.* **53**, 362 (2011).

[24] N. Birbilis, K.D. Ralston, S. Virtanen, H.L. Fraser, C.H.J. Davies, *Corros. Eng. Sci. Technol.* **45**, 224 (2010).

[25] D. Song, A. Ma, J. Jiang, P. Lin, D. Yang, J. Fan, *Corros. Sci.* **52**, 481 (2010).

[26] T. Kokubo, H. Takadama, *Biomaterials* **27**, 2907 (2006).

[27] R. Král, F. Chmelík, V. Koula, M. Rydlo, M. Janeček, *Kovove Mater.* **45**, 159 (2007).

[28] I.V. Shashkov, T.A. Lebedkina, M.A. Lebyodkin, P. Dobron, F. Chmelik, R. Kral, K. Parfenenko, K. Mathis, *Acta Phys. Pol. A* **122**, 430 (2012).

[29] M. Janeček, R. Král, P. Dobroň, F. Chmelík, V. Šupík, F. Holländer, *Mater. Sci. Eng. A* **462**, 311 (2007).

[30] I. Kralova Lesna, V. Adamkova, L. Pagacova, *Neuro Endocrinol. Lett.* **32**, Suppl 2, 24 (2011).

[31] S. Spigarelli, M.E. Mehtedi, M. Cabibbo, E. Evangelista, J. Kaneko, A. Jäger, V. Gartnerova, *Mater. Sci. Eng. A* **462**, 197 (2007).

[32] M. Janeček, S. Yi, R. Král, J. Vrátná, K.U. Kainer, *J. Mater. Sci.* **45**, 4665 (2010).

[33] P. Minárik, M. Zemková, R. Král, M. Mhaede, L. Wagner, B. Hadzima, *Acta Phys. Pol. A* **128**, 805 (2015).

[34] R.B. Figueiredo, T.G. Langdon, *J. Mater. Sci.* **44**, 4758 (2009).

[35] P. Lejcek, *Grain Boundary Segregation in Metals*, Springer Science & Business Media, 2010.

[36] O. Nejadseyfi, A. Shokuhfar, A. Dabiri, A. Azimi, *J. Alloys Comp.* **648**, 912 (2015).

[37] M.A. Abdulstaar, E.A. El-Danaf, N.S. Waluyo, L. Wagner, *Mater. Sci. Eng. A* **565**, 351 (2013).

[38] J. Orlikowski, K. Darowicki, *Electrochim. Acta* **56**, 7880 (2011).